

BIYAO GENG
WEN NI
JIAJIA WANG
XIAJIE QIU
XIAOWEI CUI
CHAO REN
SIQI ZHANG
and
YI XING

Pozzolanic reactivity and hydration products of quartz

With quartz, desulfurized gypsum and calcium hydroxide as the materials, this paper studies the pozzolanic reactivity of finely ground quartz and performs XRD, IR, DSC, NMR and SEM analysis on the hydration products of the neat paste specimens. The results show that the compressive strength of the finely ground neat quartz paste specimen is 5.66MPa and 23.49MPa respectively at the age of 3d and 28d, which indicates that the finely ground quartz has the pozzolanic reactivity, and that its main hydration product is C-S-H gel. With the curing age, C-S-H gel and zeolite-like facies continuously increase, and C-S-H gel is produced on the surfaces of quartz particles, gradually make the gaps smaller between quartz particles.

Keywords: Quartz, pozzolanic reactivity, C-S-H gel.

1. Introduction

In the 21st century, resources and energy are one of the biggest bottlenecks and constraints in economic and social development. In the national 13th five-year development plan, the core development goal “overall improvement of ecological environment quality” was proposed for the first time, which requires greatly improving the efficiency of energy resources development and utilization, promoting resource conservation and intensive use and carrying out unprecedented green revolution. As of 2013, the comprehensive utilization of coal ash in the

industrial solid waste had reached 69%, that of coal gangue 64%, and that of tailings only 18.9% [1]. Most of the oxides in the tailings are similar to the raw materials required for cement production, which makes it possible to produce building materials using these tailings. Xuan et al., [2] carried out an experimental study on sintering moderate heat portland cement with lead-zinc tailings. The results show that when lead-zinc tailings are used as ingredients, the mineral formation will be good and that the sinterability of clinker will be improved. Kutti et al., [3-4] prepared ultra-high-strength cement-based composites mixed with mineral admixtures. Some researches [5] also show that both silicate and quartz in the tailings may be involved in the reaction that generates ettringite and C-S-H gel, and that the lead-zinc tailing can be used as the active admixture of concrete. In order to further understand the role that quartz plays in the active admixture consisting of lead-zinc tailings, the paper prepares the neat paste specimen with quartz as the main material and studies the pozzolanic reactivity and hydration products of quartz, hoping to provide some bases for determining whether some tailings have pozzolanic reactivity.

2. Test materials and methods

2.1 TEST MATERIALS

- (1) Quartz: supplied by a company in Beijing. The chemical composition is shown in Table 1. It can be seen that, quartz contains up to 98.02% of SiO_2 , and also small amounts of Al_2O_3 , Fe_2O_3 and CaO . Fig.1 is the XRD spectrum of quartz.
- (2) Natural gypsum: supplied by Beijing Fangshan Shuangshan Cement Plant. The chemical composition is shown in Table 1.
- (3) Calcium hydroxide: produced by Sinopharm Chemical Reagent Co., Ltd., analytically pure.

2.2 TEST METHOD

First, use a jaw crusher to crush the quartz, and then grind it in the sampling machine for 60min to obtain finely ground

Messrs. Biyao Geng and Yi Xing, School of Energy and Environment Engineering, University of Science and Technology, Beijing, Beijing 100 083, Wen Ni, Jiajia Wang, Xiajie Qiu, Chao Ren and Siqi Zhang, Key Laboratory of Ministry of Education of China for High-Efficient Mining and Safety of Metal Mines, School of Civil and Resources Engineering, University of Science and Technology, Beijing, Beijing 100 083, Biyao Geng, Wen Ni, Jiajia Wang, Xiajie Qiu, Chao Ren and Siqi Zhang, Beijing Key Laboratory on Resource-oriented Treatment of Industrial Pollutants, Beijing 100 083, Xiaowei Cui, Shangluo College, Chemistry and Chemical Engineering, Shangluo 726 000, Biyao Geng, Beijing Weitong Environment Technology Co., Ltd., Beijing 100 144 and Biyao Geng, Beijing Yujin Resources and Environment Technology Institute, Beijing 101502, China. E-mail: niwen@ces.ustb.edu.cn

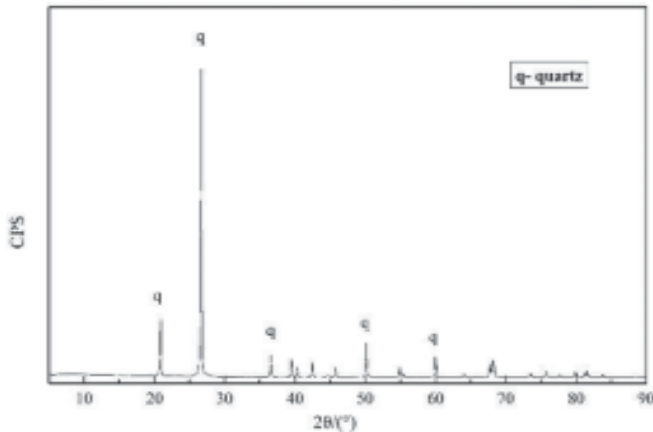


Fig.1 XRD spectrum of quartz

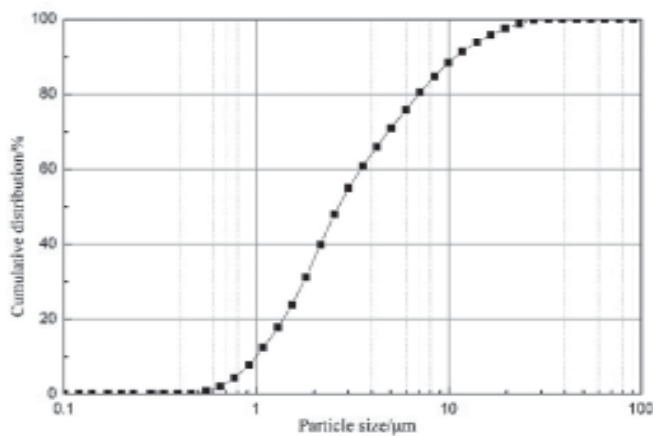


Fig.2 Particle size distribution of finely ground quartz

TABLE 1: MAIN CHEMICAL COMPONENTS OF QUARTZ (WT%)

Material	Quartz	Gypsum
SiO ₂	98.02	3.91
Al ₂ O ₃	0.80	3.61
Fe ₂ O ₃	0.05	0.19
FeO	0.36	0.33
MgO	0.00	8.94
CaO	0.065	30.93
Na ₂ O	0.00	0.15
K ₂ O	0.56	0.25
TiO ₂	0.063	0.080
P ₂ O ₅	0.007	0.017
MnO	0.059	0.081
Loss	0.12	25.49
S		26.28

quartz with a specific surface area of 782m²/kg. The particle size distribution is shown in Fig.2.

Mix finely ground quartz, natural gypsum and calcium hydroxide at a ratio of 91:3:6, and add 0.3% PC water reducer to prepare mixed dry powder (A). Then prepare a neat paste specimen with a size of 30mm×30mm×50mm, with dry powder as the raw material and at a water-binder ratio of 0.20. Perform

standard curing (at a temperature of 20±1°C and a humidity of no lower than 95%), and take samples respectively at the age of 3d, 7d and 28d, which are denoted as B1, B2 and B3. Perform XRD, SEM, DSC, IR and NMR. XRD analysis uses a Rigaku D/MAX-RC 12kW rotating anode diffractometer containing a Cu target, with a wave length of 1.5406Å, an operating voltage of 40kV, an operating current of 150mA and a scanned range of 5°<2θ<90°. The SEM analysis uses an S250 scanning electron microscope, produced by Cambridge, with an acceleration voltage of 20kV. The DSC analysis uses the differential scanning calorimeter (Netzsch STA 449C, Germany), with a temperature increasing rate of 10k/min, a temperature range of 20~1000°C, and the air as the medium. The IR analysis adopts an NEXUS70 fourier infrared spectrometer (350~7000cm⁻¹), with a resolution of 3cm⁻¹. The working conditions are: humidity 68%, temperature 27°C, frequency 56~60Hz and voltage 220~240V.

3. Analysis and discussion

3.1 COMPRESSIVE STRENGTH TEST ON THE NEAT QUARTZ PASTE SPECIMEN

Table 2 shows the test results of the compressive strength of the quartz neat paste specimen at all ages. It can be seen that the compressive strength of the neat quartz paste specimen at the age of 3d, 7d and 28d is 2.64MPa, 6.93MPa and 12.31MPa, indicating that the mechanically ground quartz has some pozzolanic reactivity.

TABLE 2: COMPRESSIVE STRENGTH OF THE NEAT QUARTZ PASTE SPECIMEN AT ALL AGES

Curing age	3d	7d	28d
Compressive strength/ MPa	2.64	6.93	12.31

3.2 XRD ANALYSIS ON THE NEAT QUARTZ PASTE SPECIMEN

Fig.3 shows the XRD test results of the mixed dry powder and neat paste specimen of quartz at all ages. As can be seen, the characteristic peak of calcium hydroxide (2θ 18.04°, 28.67°, 34.04°, 47.11° and 54.35°) is gradually weakened with

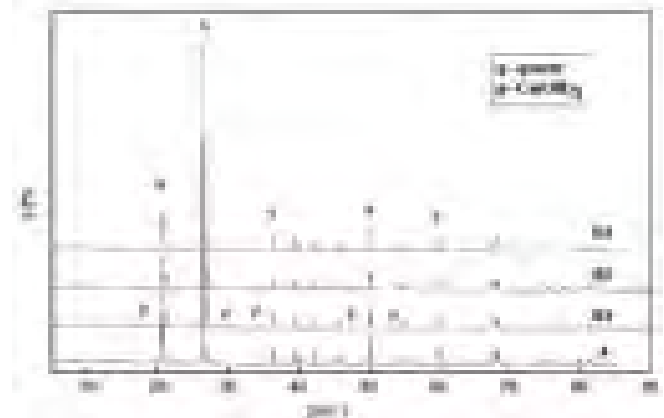


Fig.3 XRD spectra of mixed dry powder and neat paste specimen of quartz at all ages (A: dry powder, B1: 3d, B2: 7d, B3: 28d)

the age[6], until the age of 28d, when part of the peak almost disappears. Within the 2θ angle (26° - 34°) where typical C-S-H gel[7] can easily cause protrusion in the XRD spectra, in the XRD spectra of the samples in this experiment, with the curing age, the background value increases and small convex hulls appear, indicating that the C-S-H gel in the samples is on the growing trend with the curing age. The generation of C-S-H gel is the source for the strength of the neat paste specimen.

3.3 SEM ANALYSIS ON THE NEAT QUARTZ PASTE SPECIMEN

Fig.4 shows the SEM images of the neat quartz paste specimen under different magnification at all ages. Figs.4(a), (b), (c) and (d) are the images of neat quartz paste specimen at the age of 3d magnified by 5k, 20k, 50k and 100k times in the same field of vision. From Fig.4(a) and 4(b), it can be seen that, there is already C-S-H gel generated in the system at the age of 3d, and that there are large gaps between the quartz particles. Fig.4(d) shows a typical C-S-H gel structure, where there are some particles with a size of less than 100nm. However, finely ground quartz does not contain particles of such size, so it can be deduced that these are C-S-H gel particles.

Figs.5(a), (b), (c) and (d) are the images of neat quartz paste specimen at the age of 7d magnified by 5k, 20k, 50k and 100k times in the same field of vision. From Fig.5(a) and Fig.5(b), it can be seen that, the system structure is denser than that at the age of 3d, and the gaps between quartz particles are gradually narrowing. Figs.5(c) and 5(d) shows that, at the age of 7d, the C-S-H gel particles are much thicker and more solid, and the bonds between these particles are firmer and more layered.

Figs.6(a), (b) and (c) and Figs.6(d), (e) and (f) are the images of neat quartz paste specimen at the age of 28d magnified by 5k, 20k, 50k and 100k times in the same field of vision. From Figs.6(a) - 6(c), it can be seen that, the system structure is very compact at the age of 28d and that the finely ground quartz particles are already covered by massive C-S-H gel. The connections between particles are even tighter than those at the age of 3d, and the C-S-H is of wavy structure. In the center of Fig.6(d), there is a quartz particle. Figs.6(e) and 6(f) are the magnified images of the particle. As can be seen, on the surface of this particle, there are some hydration product particles with a size of less than 100nm. In this system, these hydration products should be C-S-H gel, indicating that C-S-H gel can be closely attached to the surface of the quartz particle.

3.4 FT-IR ANALYSIS ON THE NEAT QUARTZ PASTE SPECIMEN

Fig.7 is the FT-IR spectra of the mixed dry powder and neat paste specimen of quartz at all ages.

The absorption peak at the range from 3800cm^{-1} to 3000cm^{-1} is the stretching band of the O-H bond of different substances in the system, and the absorption peak at 3643cm^{-1} is the asymmetric stretching vibration absorption peak of the O-H bond in calcium hydroxide [7-10]. This absorption peak is gradually weakened with the growth of the age and almost disappears at the age of 28d, indicating that with the hydration reaction going on, the vast majority of calcium hydroxide is consumed.

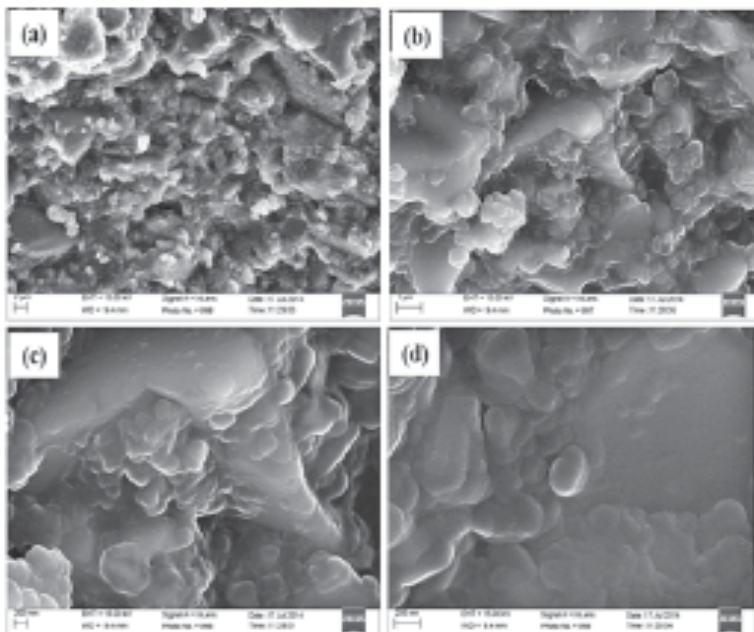


Fig.4 SEM images of the neat quartz paste specimen at the age of 3d

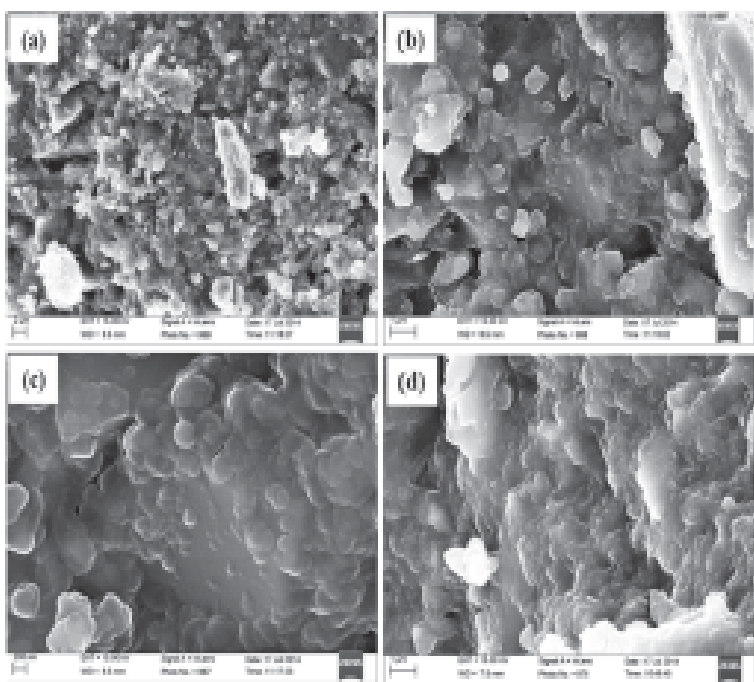


Fig.5 SEM images of the neat quartz paste specimen at the age of 7d

TABLE 3: PEAK-FIT PROCESSING RESULTS OF THE MIXED DRY POWDER AND NEAT PASTE SPECIMEN OF QUARTZ AT ALL AGES BY PEAKFIT

Age		Q ²	Q ³	Q ⁴
Mixed dry powder	Relative area	2.32	4.7	100
	Relative content (%)	2.17	4.39	93.44
3d	Relative area	3.94	12.6	100
	Relative content (%)	3.38	10.81	85.81
28d	Relative area	7.94	5.58	100
	Relative content (%)	6.99	4.92	88.09

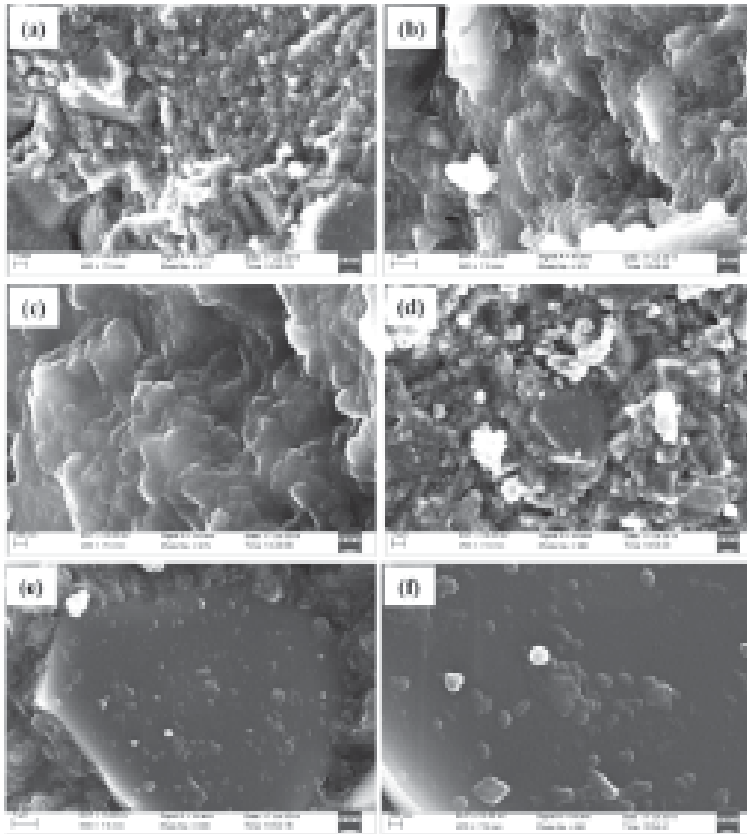


Fig.6 SEM images of the neat quartz paste specimen at the age of 28d

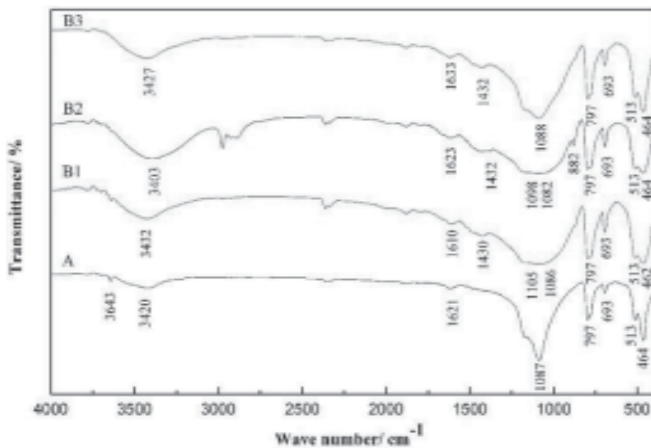


Fig.7 FT-IR spectra of mixed dry powder and neat paste specimen of quartz at all ages (A: dry powder, B1: 3d, B2: 7d, B3: 28d)

In the FT-IR spectrum of the mixed dry powder sample, the absorption peak at 3420cm^{-1} is the asymmetric stretching vibration peak of the O-H bond that connects silica [7, 11], and the surfaces of the fine particles of silicate minerals react with water molecules in the air to form such bonds. The surface of the finely ground quartz is hydroxylated when in contact with the air, which also contributes to this peak at 3420cm^{-1} . In the FT-IR spectra of the samples, at the age of 3d, 7d and 28d, the absorption peak at 3432cm^{-1} , 3403cm^{-1} and 3427cm^{-1} , respectively, is formed from the O-H bonds that connect silicon dioxide and C-S-H gel. Note that from the mixed dry powder sample to those at the age of 3d, 7d and 28d, the wave number of the peak increases, indicating that the average bond energy of the O-H bonds increases with the age, and also shows that the average gravitational force that connects the O-H bonds and the cations is continuously weakened. On the other hand, the continuous enhancement of the absorption band between 3800cm^{-1} and 3000cm^{-1} shows that the hydration reaction is ongoing with the age, which is consistent with the results obtained by XRD and SEM analysis.

The absorption peak at 1621cm^{-1} in the FT-IR spectrum of the mixed dry powder sample is the bending vibration peak of the O-H bond in the hydroxyl structural water or crystal water. In this system, the natural gypsum in the mixed dry powder sample contributes to this peak. Similar absorption peaks also appear at 1610cm^{-1} , 1623cm^{-1} and 1633cm^{-1} at the age of 3d, 7d and 28d, respectively. It can be seen from the figure that both the wave number and sharpness of the absorption peak increase with the age, indicating that the total amount of C-S-H gel is continuously increasing.

The absorption peak at 1430cm^{-1} in the spectrum at the age of 3d is the stretching vibration peak of CO_3^{2-} [7, 12], which, in this system, is caused by the carbonization reaction between the components of the mixed dry powder sample and CO_2 in the air. Similar absorption peaks also occur at 1432cm^{-1} and 1432cm^{-1} at the age of 7d and 28d, respectively. The area of the absorption peaks is increasing, indicating that, during the preparation of the sample, the sample continues to react with CO_2 in the air and undergoes carbonation.

The absorption peak at 1087cm^{-1} in the FT-IR spectrum of the mixed dry powder sample is the stretching vibration peak of the Si-O bond in the quartz and the asymmetric stretching vibration peak of the S-O bond in the natural gypsum in this system[13, 14]. Similar absorption peaks also appear at 1086cm^{-1} , 1082cm^{-1} and 1088cm^{-1} at the age of 3d,

7d and 28d, respectively. It can be seen that the sharpness of the peak decreases significantly from mixed dry powder to the sample at the age of 3d, while from 3d to 28d, the sharpness of the peak increases slightly and the peak area slightly decreases during the whole reaction, indicating that Si-O bonds in quartz exist in C-S-H gel and quartz crystals, respectively, and that the degree of order in which the siloxane tetrahedrons are arranged is low in the C-S-H gel, reducing the sharpness of the peak. With the reaction, more Si-O bonds are transferred from quartz crystals to C-S-H gel, and the degree of order in which the siloxane tetrahedrons are arranged in the C-S-H gel increases, making the sharpness of the peak recovered.

The absorption peaks near 464cm^{-1} is the asymmetric bending vibration absorption peaks of the Si-O-Si bond in silicate minerals. From the mixed dry powder sample to samples at the age of 3d, the sharpness of the absorption peak decreases, and from 3d to 28d, this peak keeps sharpening, indicating that in the beginning of the reaction, the Si-O bonds in quartz exist in C-S-H gel and quartz crystals, respectively, that the degree of order in which silica tetrahedrons are arranged in C-S-H gel is low, and that the energy distribution of Si-O-Si bonds is not concentrated, making the peak sharpness decrease. When the degree of order of the silica tetrahedrons in C-S-H gel improves and the energy distribution of Si-O-Si bonds is more concentrated, the peak will continuously sharpen.

3.5 DSC ANALYSIS ON THE NEAT QUARTZ PASTE SPECIMEN

Fig.8 shows the DSC curves of the neat quartz paste specimen at all ages. The exothermal valley at around 896.4°C is caused by the generation of β -wollastonite from C-S-H gel. Most of the endothermic peak at around 699.7°C is caused by the thermal decomposition and decarbonization of CaCO_3 generated from carbonization of $\text{Ca}(\text{OH})_2$ [15]. The endothermic peak at 576.8°C is caused by the conversion of α -quartz to β -quartz. The absorption peak at 436.7°C is caused by the decomposition of $\text{Ca}(\text{OH})_2$ [15]. This peak appears in the sample at the age of 3d. It is not obvious at the age of 7d and disappears at the age of 28d, indicating that during the hydration process, $\text{Ca}(\text{OH})_2$ is being constantly consumed and completely consumed at the age of 28d, which is consistent with the results of XRD and FT-IR analysis in section 6.4.2 and 6.4.4. The absorption peaks at 102.5°C , 101.9°C and 104.2°C are due to the dehydration of C-S-H gel[15-16]. These three absorption peaks are sharp and high, indicating that at the age of 3d, there is a considerable amount of C-S-H gel generated in the system, which is consistent with XRD, SEM and FT-IR analysis results. The weak peak at 131.2°C is due to the dehydration of hemihydrate gypsum[17], indicative of the presence of free gypsum in the sample at the age of 3d, but there are only weak indications at the age of 7d and 28d. This is also consistent with the results of XRD analysis and FT-IR analysis.

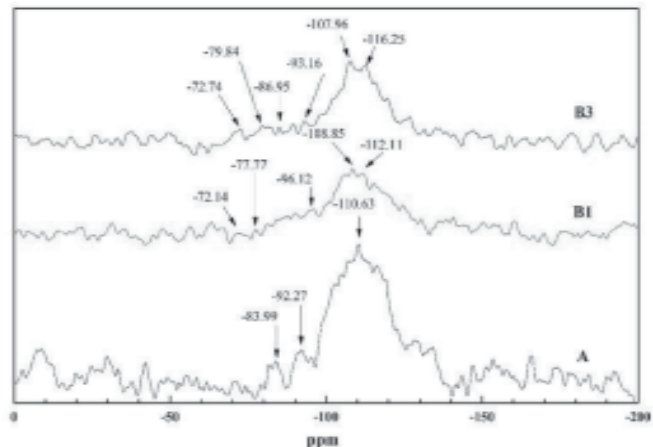


Fig.8 DSC curves of the neat quartz paste specimen at all ages (B1: 3d, B2: 7d, B3: 28d)

3.6 NMR ANALYSIS ON THE NEAT QUARTZ PASTE SPECIMEN

Fig.9 shows the ^{29}Si NMR spectra of the mixed dry powder and neat paste specimen of quartz at all ages. The peak absorption peaks of the mixed dry powder sample at -83.99ppm and -92.27ppm are the peaks of Q^2 and Q^3 [6], but pure quartz system should only contain Q^4 . The reason for this phenomenon is that, when quartz is ground to very fine powder, the specific surface area will be greatly increased, so the proportion of hydroxylated silica tetrahedrons in the system also increase significantly. In pure quartz, the ratio between silicon and oxygen should be 2:1. Each silicon atom connects four bridging oxygen ions to maintain charge balance. When quartz is ground to very fine powder, the surface will absorb the water in the air, hydroxyl ions will combine with the silicon atoms, and hydrogen ions will combine with the oxygen atoms. At this time, some parts do not need bridging oxygen connections to maintain their charge balance, and that is why Q^2 and Q^3 are present in the system.

The main absorption peak of the mixed dry powder

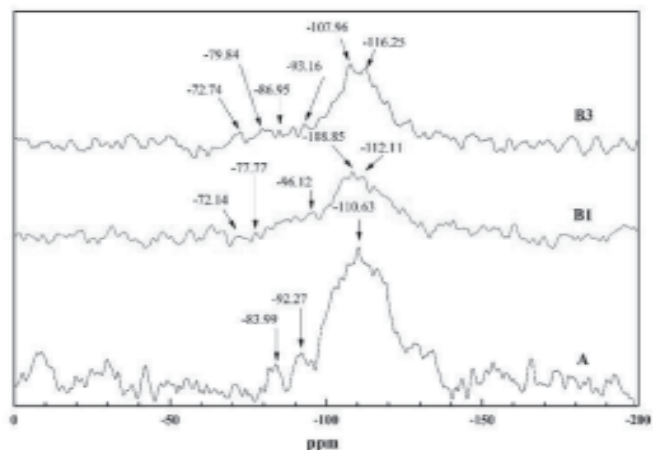


Fig.9 ^{29}Si NMR spectra of the mixed dry powder and neat paste specimen of quartz at all ages (A: dry powder, B1: 3d, B3: 28d)

at -110.63ppm is the peak of Q^4 . After mechanical activation, the 3D network structure of the particle surface Q^4 is damaged to different extents. The essence of nuclear magnetic resonance is to reflect the extranuclear electron cloud density of nucleus. In this system, when quartz is ground to very fine powder, there are a large number of near-surface and internal silicon-oxygen bonds of different angles and lengths, so the half-peak will be very wide and not sharp. The section from -98ppm to -110.63ppm is the near-surface Q^4 and that from -110.63ppm to -129ppm is the internal Q^4 . As the reaction proceeds, the height of the main peak decreases and the width of the peak increases, and the peak top is divided into two. At the age of 3d, the samples are at -108.5ppm and -112.11ppm, respectively, and at the age of 28d, the samples are at -107.96ppm and -116.25ppm. The main peak shows a trend from being concentrated in the high field to being scattered in the low field, indicating that the Q^4 content and the crystallinity in the system decrease but that the proportions of Q^0 , Q^1 , Q^2 and Q^3 increase in the system. The top of the peak is divided into two, indicating that the Q^4 in the system exists in two parts. The absorption peak at -107.96ppm is the Q^4 near the reaction layer, while the absorption peak at -116.25ppm is superimposed jointly by the Q^4 inside the quartz particles not completely reacted and the Q^4 in the zeolite-like facies[18].

The intensity of each absorption peak decreases from the dry powder sample to that at the age of 3d, but the intensity increases from 3d to 28d, indicating that in the initial reaction, the network structure of silicon-oxide polyhedrons in the system is chemically excited by hydroxyl ions, causing the bonds in the network structure to break and form single or low-polyhedral silicon polyhedra structure. Compared to the samples at the age of 3d and 28d, the intensity of Q^0 and Q^1 peaks increases and the peaks move from -72.14ppm and -77.77ppm to -72.74ppm and -79.84ppm, respectively, and the intensity of Q^3 and Q^4 peaks increases and the peaks move from -96.12ppm and -108.85ppm to -93.16ppm and -107.96ppm. The absorption peak at Q^2 changes from being not obvious to being significant at -86.95ppm, indicating that the proportion of Q^2 in the system increases and the crystallinity increases. Q^2 represents the silicon tetrahedron bonded to two silicon tetrahedrons, i.e., straight-chain or cyclic-structure silicon tetrahedron. The typical structure of C-S-H gel is precisely the chain structure, indicating that as the reaction progresses, C-S-H gel is generated in the system and its content increases with the age. This is consistent with the results of XRD, SEM, FT-IR and DSC analysis from Sections 6.4.2 through 6.4.5.

Through the peak-fit processing by the PeakFit software, the relative area and relative content of hydration products at different ages are obtained, as listed in Table 3. It can be seen that, over the age, the relative content of Q^2 increases gradually from 2.17% in the mixed dry powder to 6.99% in the sample at the age of 28d. This is because with the reaction

going, the amount of C-S-H gel continuously increases, and the main structure of C-S-H gel is chain silicate.

The relative content of Q^3 increases from 4.39% in the mixed dry powder to 10.81% in the sample at the age of 3d. This is because in the beginning of the reaction, C-S-H gel grows directly on the surface of quartz particles and the proportion of the connection between gel and quartz particles increases, which leads to the increase in the specific gravity of Q^3 . With the reaction progressing, the particle surface is being covered, that is, the amount of Q^3 is close to saturation, while the amounts of C-S-H gel and zeolite-like facies are still increasing, so the proportion of Q^3 will be relatively lower and its relative content drops to 4.92% at the age of 28d.

The relative content of Q^4 decreases from 93.44% in the mixed dry powder to 85.81% in the sample at the age of 3d, because with the reaction progressing, the amount of C-S-H gel increases in the system, lowering the proportion of Q^4 , and with the growth of age, the Q^4 in the system is divided into original Q^4 in quartz and zeolite-like facies. The increase in the total amount of the two leads to the increase in the relative content of Q^4 , which reaches 88.09% at the age of 28d. This also supports the view that in the NMR spectrum, the top of the Q^4 main peak is divided into two, i.e. Q^4 in the system exists in two forms.

4. Conclusions

- (1) The compressive strength of the finely ground neat quartz paste specimen is 5.66MPa and 23.49MPa respectively at the age of 3d and 28d, which indicates that the finely ground quartz has the pozzolanic reactivity
- (2) According to the XRD, SEM, IR, DSC and NMR analysis results of hydration products, the main hydration product of quartz is C-S-H gel. With the curing age, C-S-H gel and zeolite-like facies continuously increase, and C-S-H gel is produced on the surfaces of quartz particles, gradually making the gaps smaller between quartz particles.

Acknowledgment

The authors would like to thank the support from the National Key R&D Program of China (2017YFC0210301).

References

1. Di, Y. Q. (2015): "Preparation of high performance concrete with iron ore tailings." *Journal of Shangluo University*, vol.29, no.6, pp. 32-36, Dec.2015.
2. Xuan, Q. Q. (2009): "Lead-Zinc tailings applied in the production of moderate heat portland cement," *Journal of Materials Science and Engineering*, vol.27, no.2, pp.266-270, Apr.2009.
3. Kutti, T., Malinowski, R. and Srebnik, M. (1983): "Investigation of mechanical properties and structure of alkaline activated blast-furnace slag mortars." *Silicon Industry*, vol.9, pp.175-181, 1983.

4. Moallah, M. Y. A., Hess, T. R., Tsai, Y. N. and Cocke, D. L. (1993): "An FTIR and XPS investigation of the effects of carbonation on the solidification/stabilization of cement based system-Portland Type V with zinc." *Cement and Concrete Research*, 23(4), pp.773-784, 1993.
5. Geng, B. Y., Ni, W. and Wang, J. J. (2015): "An Initiative Investigation of the Pozzolanic Reaction of Ground Lead-Zinc Ore Tailings," *International Journal of Earth Sciences and Engineering*, vol.8, no.3, pp.1271-1278, 2015.
6. Yang, N. R. and Yue, W. H. (2000): "Atlas manual of inorganic non-metallic materials." Wuhan, China: Wuhan University of Technology Press, 2000.
7. Ylmén, R., Jäglid, U. and Steenari, B. M. (2009): "Early hydration and setting of Portland cement monitored by IR, SEM and Vicat techniques." *Cement and Concrete Research*, vol. 39, no. 5, pp. 433-439, 2009.
8. Silva, D. A., Roman, H. R. and Gleize, P. J. P. (2002): "Evidences of chemical interaction between EVA and hydrating Portland cement," *Cement and Concrete Research*, vol. 32, no. 9, pp.:1383-1390, 2002.
9. Lee, T. C., Wang, W. J. and Shih, P. Y. (2009): "Enhancement in early strengths of slag-cement mortars by adjusting basicity of the slag prepared from fly-ash of MSWI." *Cement and Concrete Research*, vol. 39, no. 8, pp. 651-658, 2009.
10. Mollah, M. Y. A. (2000): "A Fourier transform infrared spectroscopic investigation of the early hydration of Portland cement and the influence of sodium lignosulfonate." *Cement and Concrete Research*, vol. 30, no. 2, pp.267-273, 2000.
11. Peng, W. S. and Liu, G. K. (1991): "Infrared spectra of gypsum and its thermal transformation products." *Acta Mineralogical Sinica*, vol.11, no.1, pp.27-32, 1991.
12. Trezza, M. A. and Lavat, A. E. (2001): "Analysis of the system $3\text{CaO}\cdot\text{Al}_2\text{O}_3\text{-CaSO}_4\cdot 2\text{H}_2\text{O-CaCO}_3\text{-H}_2\text{O}$ by FT-IR spectroscopy," *Cement and Concrete Research*, vol. 31, no. 6, pp.869-872, 2001.
13. Lodeiro, I. G., Macphee, D. E., Palomo, A. and Fernández-Jiménez, A. (2009): "Effect of alkalis on fresh C-S-H gels. FTIR analysis," *Cement and Concrete Research*, Vol. 39, no. 3, pp.147-153, 2009.
14. Zhu, Z. X. (1988): "Infrared spectrum research on garnets and clinopyroxenes in skarn lead-zinc." *Journal of Changchun University of Earth Science*, vol.18, no.4, pp.410-414, 1988.
15. Alexander, V. S., Lionel, J. J. C. and Stephen, D. K. (2013): "A combined QXRD/TG method to quantify the phase composition of hydrated Portland cements," *Cement and Concrete Research*, vol. 48, pp. 17-24, 2013.
16. Carmona-Quiroga, P. M. and Blanco-Varela, M. T. (2013): "Ettringite decomposition in the presence of barium carbonate," *Cement and Concrete Research*, vol. 52, pp.140-148, 2013.
17. Gomes, S., François, M. and Pellissier, C. (1998): "Characterization and comparative study of coal combustion residues from a primary and additional flue gas secondary desulfurization process," *Cement and Concrete Research*, vol. 28, no. 11, pp. 1605-1619, 1998.
18. He, Y. J. and Hu, S. G. (2007): "Application of ^{29}Si Nuclear Magnetic Resonance (NMR) in Research of Cement Chemistry." *Journal of Materials Science and Engineering*, vol.25, no.1, pp.147-153, 2007.

STUDY ON EFFECTS OF PLATEAU ENVIRONMENT ON MINE FANS' PARAMETERS OF CHARACTERISTIC CURVES

Continued from page 718

- [9] Wang, X.D., Hu, N.L., & Li, G.Q. (2014): "Optimized design of ventilation in long-distance dead end of plateau mines," *International Journal of Earth Sciences and Engineering*, vol. 7, no. 3, pp. 901-906, 2014.
- [10] Jia, J.Z., Zhou, X.H., & Liu, J. (2000): "The determination of the optimal power of data fitting to characteristic curve of the fan," *Journal of Liaoning Technical University*, vol.19, no.5, pp. 478-480,2000.
- [11] Lv, M.C., Hua, G., Liu, F., & Fang, L.G. (2011): "Visualization research of characteristics curve fitting based on least Squares," *Coal Mine Machinery*, vol. 32, no. 6, pp. 85-87, 2011.
- [12] Lv, Y.D., & Tan, L. (2000): "Climatic characteristics at altitude and its physiological influences," *Science of Travel Medicine*, vol.6, no.1, pp.13-18,2000.
- [13] Chai, Z.J., Yu, M., & Zeng, Y. (2004): "Plateau reaction research on quick-Reaction force," *Journal of The Fourth Military Medical University*, vol.25, no.8, pp. 749-751, 2004.
- [14] Li, Y.L. (2000): "Effects of high altitude hypoxia on human physiology," *Journal of Qinghai Normal University*, vol. 2, no. 2, pp. 62-65, 2000.
- [15] Qiao, H.T. (2008): "Discussion on selection of main fan in mine," *Colliery Mechanical & Electrical Technology*, vol. 1, no. 6, pp. 84-86, 2008.